euspen's 20th International Conference & Exhibition, Geneva, CH, June 2020
www.euspen.eu

Grejda optimization for radial, tilt, and face error motion of an air bearing spindle

Byron Knapp, Dave Arneson, and Dan Oss

Professional Instruments Company, Hopkins, Minnesota USA

bknapp@airbearings.com

Abstract
For applications that require spindles with nanometer-level radial and face error and nanoradian-level tilt accuracy, the orientation of the spindle can play an important role. In this work, the Grejda optimum orientation angle is determined for radial, tilt and face error of an air bearing spindle. Using two orthogonal measurements of radial error, the fixed sensitive direction radial spindle error is found for every spindle orientation. Tilt error at every orientation angle is determined with two more radial measurements. Combining the axial measurement with the tilt, face error as a function of orientation angle is calculated. Compared to the maximum errors, Grejda optimum orientation angles provide a 37% improvement radial, 26% improvement tilt, and a 24% improvement in face error motion on a 100 mm radius. These optimum synchronous error motion values can be realized simply by correctly positioning the spindle stator during spindle installation at 106° for optimum radial, 50° for optimum tilt, or 31° for optimum face on a 100 mm radius.

Spindle error motion, Grejda optimization, spindle metrology

1. Introduction

The most demanding manufacturing and metrology applications require spindles with nanometer-level spindle error motion. Achieving this level of accuracy requires continued advances in precision manufacturing, tooling, assembly, and metrology. However, many are unaware of a simple solution for improved error motion using a spindle's optimum orientation angle. While the concept was introduced in the B89.3.4 Standard [1], the benefit was first demonstrated for radial error by Grejda [2]. This paper extends Grejda optimization by determination of the orientation angles that yield the lowest errors for radial, tilt, and face error motion for an air bearing spindle.

2. Methodology

The benefits of combining multiprobe error separation with Grejda optimization for synchronous radial error motion has been previously described [3]. With two orthogonal measurements in a plane normal to the axis of rotation, the fixed sensitive direction radial error at any orientation can be calculated using Equation 1.

$$R(\theta) = \Delta X_1(\theta)cos\phi + \Delta Y_1(\theta)sin\phi \quad (1)$$

Where $R(\theta)$ is fixed sensitive radial error motion at an orientation angle ϕ, θ is angular position of the axis of rotation, $\Delta X_1(\theta)$ and $\Delta Y_1(\theta)$ are the two orthogonal separated radial spindle error results at orientation angles 0° and 90°. Multiprobe error separation is used to obtain the spindle error components necessary to solve Equation 1. Illustrated in Figure 3, Equations 2-4 are solved for the artifact form error, $F(\theta)$, and spindle errors $\Delta X(\theta)$ and $\Delta Y(\theta)$ using the technique described by Marsh [4].

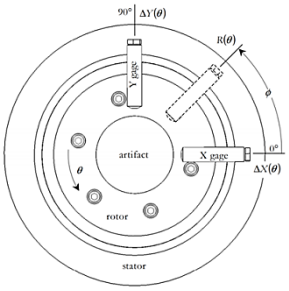

Figure 1. Using $\Delta X(\theta)$ and $\Delta Y(\theta)$, the spindle error for any orientation angle ϕ can be calculated [2].

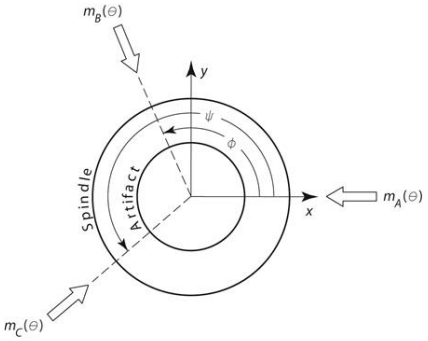

Figure 2. Multiprobe error separation uses three asymmetrically orientated measurements to separate artifact and spindle error [4].

$$m_A(\theta) = F(\theta) + \Delta X(\theta)sin\phi \quad (2)$$

$$m_B(\theta) = F(\theta - \phi) + \Delta X(\theta)cos\phi + \Delta Y(\theta)sin\phi \quad (3)$$

$$m_C(\theta) = F(\theta - \psi) + \Delta X(\theta)cos\psi + \Delta Y(\theta)sin\psi \quad (4)$$

The tilt error for any orientation angle is calculated according to Equation 5.

$$\alpha(\theta) = \alpha_X(\theta)cos\phi + \alpha_Y(\theta)sin\phi \quad (5)$$

Where $\alpha(\theta)$ is fixed sensitive tilt error motion at an orientation angle ϕ, θ is angular position of the axis of rotation, $\alpha_X(\theta)$ and $\alpha_Y(\theta)$ are the two orthogonal components of tilt error calculated from radial measurements with known spacing as shown in Equations 6 and 7.

$$\alpha_X(\theta) = \frac{\Delta X_2(\theta) - \Delta X_1(\theta)}{L} \quad (6)$$

$$\alpha_Y(\theta) = \frac{\Delta Y_2(\theta) - \Delta Y_1(\theta)}{L} \quad (7)$$

Where $\Delta X_1(\theta)$ and $\Delta Y_1(\theta)$ are the spindle radial errors at the first axial location, $\Delta X_2(\theta)$ and $\Delta Y_2(\theta)$ are the radial errors a second axial location at a known distance L from the first set.

Lastly, the combining the axial error with the tilt error, the face error can be calculated according to Equaton 8:

$$F(\theta) = Z(\theta) + \alpha(\theta) \cdot d \quad (8)$$

Where $F(\theta)$ is the face error at a radius d, and $Z(\theta)$ is the axial error motion.

3. Approach

The air bearing spindle in this work is shown in Figure 3. It is a Blockhead Model 10R-606 featuring high stiffness and nanometer-level error motions within a compact footprint. With an inlet air pressure of 0.7 MPa, radial stiffness is better than 0.35 kN/µm and axial stiffness is better than 0.6 kN/µm. Radial and axial synchronous errors are less than 25 nm and tilt error is better than 0.1 µrad. The spindle has a 154 mm diameter clear aperture making it suitable to a wide range of applications including as an alignment tool for optical assemblies.

Figure 3. The air bearing spindle in this work—Blockhead 10R-606.

The assembly shown in Figure 4 includes a frameless, brushless permanent magnet servo motor and high resolution encoder. The motor (Aerotech S-240) is designed for minimal parasitic errors using slotless aluminum laminations combined with reduced gap flux and a sinusoidal flux profile. A linear amplifier (Aerotech HLe-10-40) is chosen to minimize current ripple and radiated electrical noise. The encoder has a 20 µm pitch grating on a 209 mm diameter ring with 32,768 lines (Renishaw RESM). The analog output enables highly interpolated resolution and a graduation accuracy of ±1 arc second.

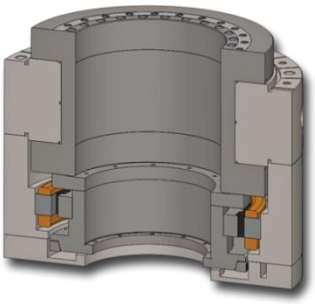

Figure 4. Cross section of the motorized spindle assembly.

The synchronous spindle error components $\Delta X_1(\theta)$, $\Delta Y_1(\theta)$, and $Z(\theta)$ are obtained using the setup shown in Figure 5 for 10 revolutions at 120 RPM. A capacitive sensor (Lion Precision C23-C) targets a 25 mm diameter lapped sphere. The sensor amplifier (Lion Precision CPL190) incorporates a 15 kHz first-order, low-pass analog filter with linear phase response. The data acquisition system (Lion Precision SEA) is triggered by the divided encoder signal (32x divider providing 1,024 points per revolution), providing immunity to synchronization errors caused by speed variation. Bespoke tooling is used to position a single sensor to three angular orientations chosen to minimize harmonic distortion through 225 UPR (0°, 99.844° and 202.5°). The tooling also permits shifting each of the measurements 90° for the orthogonal error component. Then, Equations 2-4 are solved to extract the target error from the desired radial synchronous spindle error. The axial error measurement does not require error separation. A low-pass digital filter with a 150 UPR cut-off is applied to the radial and axial results.

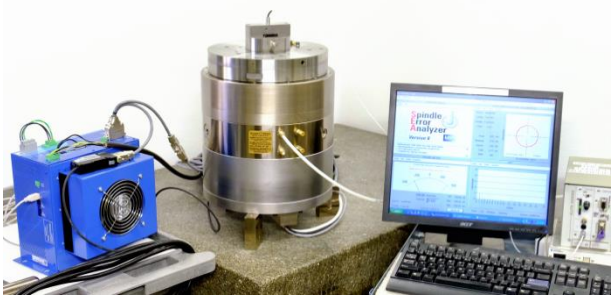

Figure 5. Test setup with motorized spindle, bespoke tooling, and data acquisition system. Low ball is 225 mm up from the spindle center.

A second set of radial measurements at a known distance from the first set is required to obtain the tilt error. The two sets of the measurements are commonly referred to as “low ball” and “high ball.” The low ball measurements are 225 mm up from the center of the spindle. The high ball setup shown in Figure 6 is 375 mm from the center of the spindle using a 150 mm riser for the target and the probe holder. Again using multiprobe separation and bespoke tooling, the synchronous spindle error components $\Delta X_2(\theta)$ and $\Delta Y_2(\theta)$ are found.

Figure 6. High ball test measuring radial errors 375 mm up from the center of the spindle.

4. Results

Synchronous radial spindle error results are shown in Figure 7. The radial error in the X direction is 18.2 nm and the radial error in the Y direction is 12.9 nm. It is interesting to note that the X direction error is dominated by 3-lobe error but the Y direction is primarily 2-lobed. These orthogonal error components $\Delta X_1(\theta)$ and $\Delta Y_1(\theta)$ are used in Equation 1 to calculate $R(\theta)$, the radial error motion as a function of orientation angle ϕ. The predicted error curve in Figure 5 is only plotted for orientation angles from 0°-180° since measurements from 180°-360° are identical but with a change of sign [2]. The maximum error is 18.4 nm and occurs at 8° whilst the minimum is 11.6 nm at 106°. Although it may not be practical to install the spindle at the exact minimum orientation angle, any orientation angle from 75°-150° will provide radial error that is lower than the average.

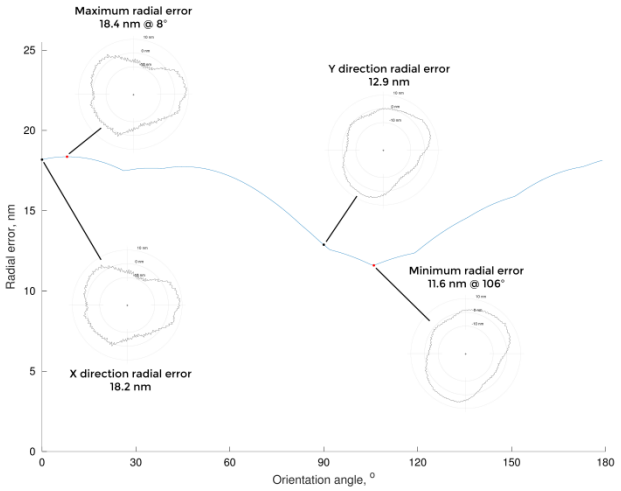

Figure 7. Radial error as a function of orientation angle. The Grejda optimum is 11.6 nm at 106°. The radial error specification for the 10R-606 at 225 mm up from the spindle center is 47.5 nm (including the contribution from tilt).

The axial error measurement is also obtained from the setup shown in Figure 5. The sensor is placed coaxially with the spindle axis of rotation in the probe holder targeting the top of the artifact. Unlike radial error, axial error measurement does not require error separation. Further, fundamental axial motion is an error of the axis and is included in the result. The synchronous axial error $Z(\theta)$ measured for this assembly is 4.9 nm as shown in Figure 8.

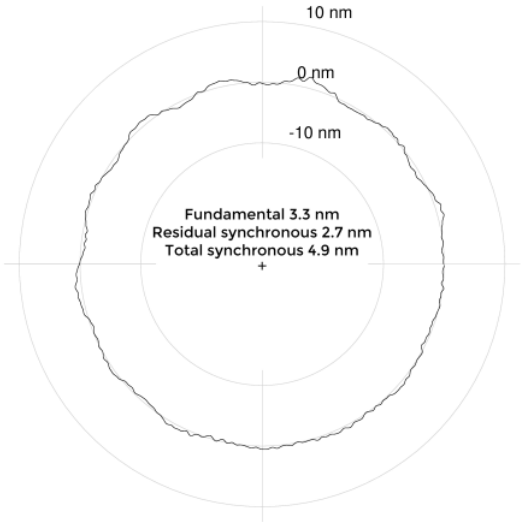

Figure 8. Axial error motion with 3.3 nm fundamental, 2.7 nm residual, and 4.9 nm total synchronous.

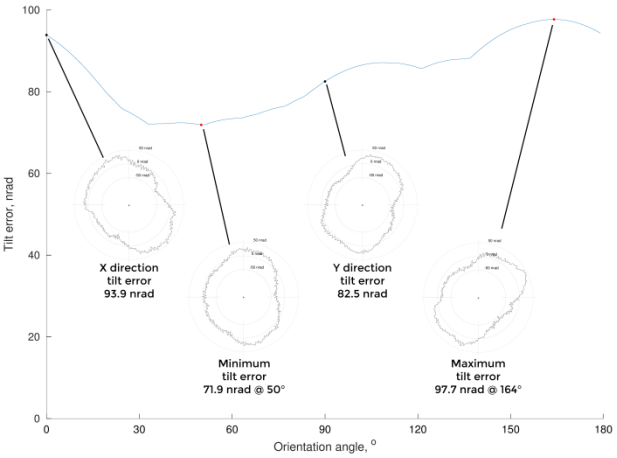

Figure 9. Tilt error as a function of orientation angle. The Grejda optimum is 71.9 nanoradians at 50°. The tilt specification is 100 nrad.

The orthogonal error components $\Delta X_2(\theta)$ and $\Delta Y_2(\theta)$ are calculated from measurements obtained in the high ball setup shown in Figure 6. With these components, the X and Y direction components of tilt error $\alpha_X(\theta)$ and $\alpha_Y(\theta)$ are calculated using Equations 6 and 7.

The tilt error results are shown in Figure 9. The tilt error in the X direction is 93.9 nanoradians and the tilt error in the Y direction is 82.5 nanoradians. Using Equation 5, the tilt error as a function of orientation angle is calculated. The maximum error is 97.7 nanoradians and occurs at 164° whilst the minimum is 71.9 nanoradians at 50°. The zone of lower than average tilt error occurs over orientation angles from 25°-90°.

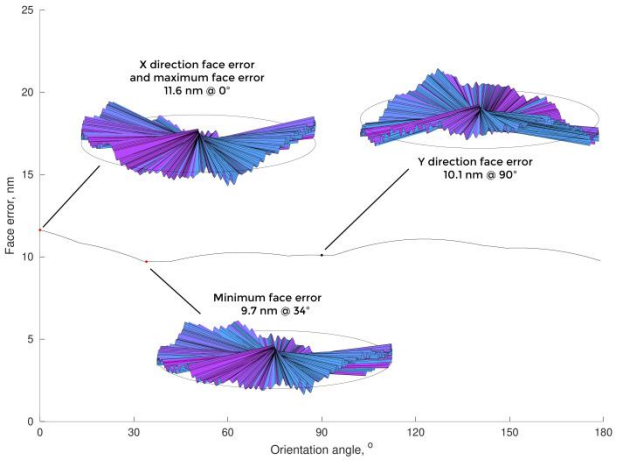

Figure 10. Face error as a function of orientation angle on a 100 mm radius. The Grejda optimum is 9.7 nm at 34°. The face error specification for the 10R-606 at a radius of 100 mm is 35 nm (including the contribution from tilt).

Combining the tilt results with the axial result, the face error at a given radius is calculated according to Equation 8. The face results at a radius of 100 mm are shown in Figure 10. The face error in the X direction is 11.6 nm and the face error in the Y direction is 10.1 nm. In this case, the maximum face error occurs at 0° degrees, coinciding with the X direction. The face error at the Grejda optimum orientation angle is 9.7 nm at 34°. The lowest face errors occur from 30°-90°.

4. Summary

Grejda optimization is a simple solution to realize the lowest possible spindle error at the optimum orientation angle. In this work, multiprobe separation is used to extract the orthogonal components of spindle error. These components are used to calculate the radial, tilt, and face error motion for an air bearing spindle as a function of orientation angle. In this case, the maximum radial error is 18.4 nm at 8° while the optimum orientation of 106° yields 11.6 nm. The novel aspect of this work was determining the Grejda optimum for tilt and face error. The maximum tilt error is 97.7 nrad at 164° but the minimum is 71.9 nrad at 50°. Lastly, the face error on a 100 mm radius is calculated with the maximum at 0° of 11.6 nm and the minimum at 34° of 9.7 nm. These findings are important because during installation of the spindle, the optimum orientation of the stator can be chosen to minimize a desired error component.

5. Conclusion

In order to realize the lowest possible spindle errors, the orientation of the spindle stator is critical. The optimum synchronous error motion is realized simply by correctly orienting the spindle during installation.The benefits of this technique were first demonstrated by Grejda for radial error and extended to tilt and face error in this work. In the case of this work, Grejda optimum orientation angles provide a 37% improvement radial, 26% improvement tilt, and a 24% improvement in face error motion on a 100 mm radius.

References

[1] ANSI/ASME B89.3.4 2010 *Axes of Rotation; Methods for Specifying and Testing*. (New York: ASME)

[2] Grejda RD 2002 *Use and calibration of ultraprecision axes of rotation with nanometer level metrology* (University Park, PA: The Pennsylvania State University)

[3] Knapp B, Arneson D, Oss D 2018 Using Grejda optimization to determine the best orientation of a spindle *Proc. ASPE*

[4] Marsh ER 2010 *Precision Spindle Metrology, Second Edition* (Lancaster, PA: Destech Publications, Inc.)